other activated or inflammatory cell populations. Nevertheless, our data establish that iNOS is distinct from cNOS. The two enzymes shared only 51% of their amino acid sequence and polyclonal antibody to iNOS did not react with recombinant rat cerebellar cNOS (*12*). Amino acid identity between iNOS and cNOS was high in regions provisionally identified as important for the binding of FAD and the reduced form of $NADP^+$ (NADPH), cofactors for which the two enzymes have similar requirements, but considerably less in the region presumed to bind calmodulin, for which the requirements of the enzymes differ dramatically.

Members of the NOS family appear to be better distinguished by their mode of activation than by the organ or cell type of their origin. Every organ is a mixture of cell types that includes endothelium (prototypic host cells for cNOS) and macrophages (prototypic host cells for iNOS) (*1*) and thus is likely to contain both enzymes under some circumstances. Even the same cell population may contain both a constitutive, agonist-activated, rapidly responsive, low-output NOS activity and a slowly induced, immunologically elicited, high-output NOS activity, perhaps reflecting the presence of both cNOS and iNOS within a single cell (*13*). Although cNOS is activated by elevation of intracellular Ca^{2+}, the major mechanism for activation of iNOS appears to be transcriptional induction.

REFERENCES AND NOTES

1. S. Moncada, R. M. J. Palmer, E. A. Higgs, *Pharmacol. Rev.* **43**, 109 (1991); L. J. Ignarro, *Biochem. Pharmacol.* **41**, 485 (1991); J. B. Hibbs, Jr., *et al.*, *Nitric Oxide from L-Arginine: A Bioregulatory System*, S. Moncada and E. A. Higgs, Eds. (Elsevier, Amsterdam, 1990), pp. 189–223; C. Nathan and J. B. Hibbs, Jr., *Curr. Opin. Immunol.* **3**, 65 (1991); D. J. Stuehr and O. W. Griffith, *Adv. Enzymol. Relat. Areas Mol. Biol.*, in press; Q.-w. Xie and C. Nathan, in *Cellular and Molecular Mechanisms of Inflammation*, C. Cochrane and M. Gimbrone, Eds. (Academic Press, New York, in press).
2. D. S. Bredt and S. H. Snyder, *Proc. Natl. Acad. Sci. U.S.A.* **87**, 682 (1990).
3. R. Busse and A. Mülsch, *FEBS Lett.* **265**, 133 (1990).
4. D. J. Stuehr, H. J. Cho, N. S. Kwon, M. F. Weise, C. F. Nathan, *Proc. Natl. Acad. Sci. U.S.A.* **88**, 7773 (1991).
5. D. S. Bredt *et al.*, *Nature* **351**, 714 (1991).
6. T. D. Porter, *Trends Biochem. Sci.* **16**, 154 (1991).
7. P. A. Karplus, M. J. Daniels, J. R. Herriott, *Science* **251**, 60 (1991); K. O. Elliston and M. W. Baum, unpublished observations; T. D. Lee *et al.*, in preparation.
8. Y. Yui *et al.*, *J. Biol. Chem.* **266**, 12544 (1991).
9. K. T. O'Neil and W. F. DeGrado, *Trends Biochem. Sci.* **15**, 59 (1990).
10. D. J. Stuehr *et al.*, *Biochem. Biophys. Res. Commun.* **161**, 420 (1989).
11. I. J. Amber, J. B. Hibbs, Jr., R. R. Taintor, Z. Vavrin, *J. Leukocyte Biol.* **44**, 58 (1988).
12. Q.-w. Xie *et al.*, unpublished observations.
13. S. Lamas, T. Michel, B. M. Brenner, P. A. Marsden, *Am. J. Physiol.* **261**, C634 (1991).
14. The RAW 264.7 murine macrophage cell line was activated with recombinant IFN-γ (rIFN-γ) (100 U/ml; Genentech, San Francisco, CA) and LPS (2 μg/ml) for 4 hours. Polyadenylated RNA with oligo(dT) as a primer was used to prepare a cDNA library in the Uni ZAP-XR unidirectional vector (Stratagene). Antiserum was raised by injecting a rabbit with 90 μg of 130-kD iNOS that was purified as described (*4*) from two 100-liter cultures of activated RAW 264.7 cells and emulsified with Freund's complete adjuvant, followed by two booster injections of incomplete Freund's adjuvant that contained 45 to 50 μg each of iNOS that was purified as above and additionally by isolation of the 130-kD region on SDS–polyacrylamide gel electrophoresis. Immunoglobulin G (IgG) antibody to iNOS was purified on immobilized recombinant protein G (Pierce), adsorbed with *Escherichia coli*, and used to screen the cDNA library.
15. M. Kozak, *J. Biol. Chem.* **266**, 19867 (1991).
16. Abbreviations for the amino acid residues are: A, Ala; C, Cys; D, Asp; E, Glu; F, Phe; G, Gly; H, His; I, Ile; K, Lys; L, Leu; M, Met; N, Asn; P, Pro; Q, Gln; R, Arg; S, Ser; T, Thr; V, Val; W, Trp; and Y, Tyr.
17. S. A. McLuckey, G. J. van Berkel, G. L. Glish, E. C. Huang, J. D. Henion, *Anal. Chem.* **63**, 375 (1991).
18. T. D. Lee and S. Vemuri, *Biomed. Environ. Mass Spectrom.* **19**, 639 (1990).

19. We thank P. Davies, A. Williamson, and J. Schmidt for advice; M. A. Palladino, Jr., and Genentech for rIFN-γ; K. Elliston and M. Baum for homology analysis; J. Aunins, C. Seamans, L. Egger, K. Glazomitsky, S. Grant, M. Silberklang, and M. Weise for their contributions to the scaled-up purification of iNOS; D. Stuehr for lysate of cNOS-transfected cells; J. B. Hibbs, Jr., for EMT-6 cells; S. Grant for rat peritoneal neutrophils; and J. MacMicking for review of the manuscript. Supported in part by NIH grants CA43610 and AI30165.

23 December 1991; accepted 25 February 1992

Chromosome Size-Dependent Control of Meiotic Recombination

David B. Kaback,* Vincent Guacci,† Dianna Barber, James W. Mahon

Smaller chromosomes have higher rates of meiotic reciprocal recombination (centimorgans per kilobase pair) than larger chromosomes. This report demonstrates that decreasing the size of *Saccharomyces cerevisiae* chromosomal DNA molecules increases rates of meiotic recombination and increasing chromosome size decreases recombination rates. These results indicate that chromosome size directly affects meiotic reciprocal recombination.

During meiosis I, homologous chromosomes pair, undergo reciprocal recombination (crossing-over), and then segregate from each other to reduce the number of chromosomes by half. Crossing-over is believed to be required to ensure proper pairing and segregation. Accordingly, in most organisms there is at least one crossover event between each pair of homologous chromosomes (*1*).

The total length of a chromosome's genetic map is a function of the total amount of meiotic reciprocal recombination on that chromosome. Genetic map lengths determined for most of the 16 chromosomes from the yeast *Saccharomyces cerevisiae* are close to complete and vary from 150 to 450 centimorgans (cM), indicating an average of three crossovers per meiosis for the smallest chromosome [250 kilobases (kb)] to nine crossovers for the largest [1650 kb, exclusive of the chromosome that contains ribosomal DNA (rDNA) because rDNA does not undergo meiotic recombination (*2, 3*)] (*4, 5*). From these results, it was concluded that DNA sequences on the smallest yeast chromosome must undergo recombination at a twofold higher average rate (0.6 cM/kb) than DNA sequences on the largest (0.3 cM/kb) (*4, 5*).

The mechanism enabling small *S. cerevisiae* chromosomes to undergo meiotic recombination at high rates is not understood. Various chromosomal sequences have been shown to undergo meiotic recombination at different rates, suggesting specific sequences may be involved in controlling recombination (*5–8*). However, the smallest yeast chromosome has a high recombination rate over most of its physical length (*5*), suggesting that chromosome size also may play a role.

To investigate the role of chromosome size in regulating meiotic recombination, we used strains in which the 250-kb chromosome *I* DNA molecule was bisected into functional half-chromosomes (*9*) (Fig. 1). Chromosome *I* was bisected at *CEN1*, producing chromosomes *IL* and *IR* that were 150 and 100 kb, respectively. Chromosome *I* also was bisected near the *MAK16* gene, giving chromosomes *IA* and *IB* that were 125 and 135 kb, respectively. Genetic markers were crossed onto each set of bisected chromosomes to enable measurement of recombination over large regions (Fig. 1A). Pulse-field gel electrophoresis (PFGE) confirmed that the marked strains contained

Department of Microbiology and Molecular Genetics, Graduate School of Biomedical Sciences, University of Medicine and Dentistry of New Jersey–New Jersey Medical School, 185 South Orange Avenue, Newark, NJ 07103.

*To whom correspondence should be addressed.
†Present address: Department of Embryology, Carnegie Institution of Washington, Baltimore, MD 21210.

only bisected copies of chromosome *I* (Fig. 1B). Diploids homozygous for each chromosome *I* bisection were constructed from the marked strains (Table 1). As a control, chromosome *I* was reconstituted by homologous recombination between the fragments in each haploid parent of all diploids described above (9). Recombinants were analyzed by PFGE to show that chromosome *I* was full length (Fig. 1B). Mating these haploids yielded isogenic diploids containing intact copies of chromosome *I*.

Diploids were sporulated to induce meiosis and the resultant asci were analyzed. Tetrad analysis (Tables 1 and 2) indicated that the recombination map distance over most of chromosome *I* was higher in all diploids containing the homozygous bisected chromosomes than in the isogenic controls containing full-length chromosomes. Recombination map distances in the controls were not significantly different from the published values. The recombination "hot-spot" defined by the *CDC24-PYK1* interval (*5, 10*) showed a proportional increase in crossovers in the bisection. In both bisections, the 17-kb *CEN1-ADE1* interval adjacent to the centromere showed no increase compared to the controls. However, *CEN1-ADE1* recombination in the controls was higher than the published value. Therefore, we cannot be certain whether there was a size-related effect in this region. Totaling the recombination map distances between all appropriate markers indicated that the recombination rate on chromosome *I* was 84% higher in strains containing the homozygous *CEN1* bisection chromosomes and 40% higher in strains containing the homozygous *MAK16* bisection chromosomes than in the full-length controls.

These analyses also confirmed the bisection and reconstitution of chromosome *I*. Markers on one-half of chromosome *I* showed no linkage to markers on the other half in bisection strains. Parental ditype (PD) asci equaled nonparental ditype (NPD) asci for *PYK1-ADE1*, *MAK16-ADE1*, or *CDC24-FUN30*. In contrast, PD asci were more numerous than NPD asci for these gene pairs in the controls, indicating that linkage was restored when chromosome *I* was reconstituted (Table 1).

To further investigate the effect of chromosome size on recombination, we constructed a chromosome *I*–chromosome *II* reciprocal translocation by the method of Fasullo and Davis (*11*) that placed chromosome *I* sequences on much larger 450- and 650-kb DNA molecules (Fig. 2A). Crosses between the translocation strain and normal strains marked on chromosome *I* yielded appropriately marked haploids that were shown by PFGE to contain the translocation (Fig. 2B). As a control, identically marked congenic strains containing normal chromosomes were obtained from these same crosses. Haploids were mated, yielding diploids that were either homozygous for the translocation chromosomes or homozygous for normal chromosomes. Tetrad analysis of these diploids indicated that four out of five intervals, including the *CDC24-PYK1* "hot-spot," showed significantly decreased recombination map distances in the translocation strains (Table 3). In total, there was 34% less reciprocal recombination when chromosome *I* sequences were contained on larger DNA molecules. No significant change was found for the *CEN1-ADE1* interval, suggesting that this region is not directly affected by chromosome size. Because centromeres inhibit recombination (*12*), this effect may be dominant over the effect produced by chromosome size.

Gene conversions were monitored in all bisection and translocation experiments (Tables 2 and 4). The number of observed events was too low to affect any of our conclusions. In addition, the numbers were also too low and too variable to indicate any size-related changes in this form of recombination.

To determine whether reciprocal recombination was affected on other chromosomes, we monitored crossovers in the *CEN3-MAT* interval on chromosome *III* (*13*) in strains carrying the chromosome *I* bisections, the translocations, and most of the controls. No significant changes from the published values were observed, indicating other chromosomes were not affected (Tables 1 and 3).

We also examined *CEN3-MAT* in a strain derived from 353-14A, which contains homozygous bisected copies of chromosome *III* (*14*) to determine if the size-related effects on recombination were generalizable to other chromosomes. In these strains, chromosome *III* was bisected to give 240- and 120-kb functional half-chromosomes. Recombination in the bisection was compared to congenic controls derived from strain 353-14ALU containing full-length copies of chromosome *III* (*14*). Similar to the chromosome *I* bisections, reciprocal recombination was 50% higher in the homozygous chromosome *III* bisection strain (FDS:SDS; 27:61 = 34.7 cM for the bisection versus 69:60 = 23.3 cM for the full-length chromosomes). Interestingly, a heterozygous diploid containing a chromosome *III* bisection and a wild-type copy of chromosome *III* showed an increased rate of recombination (*14*), suggesting that the

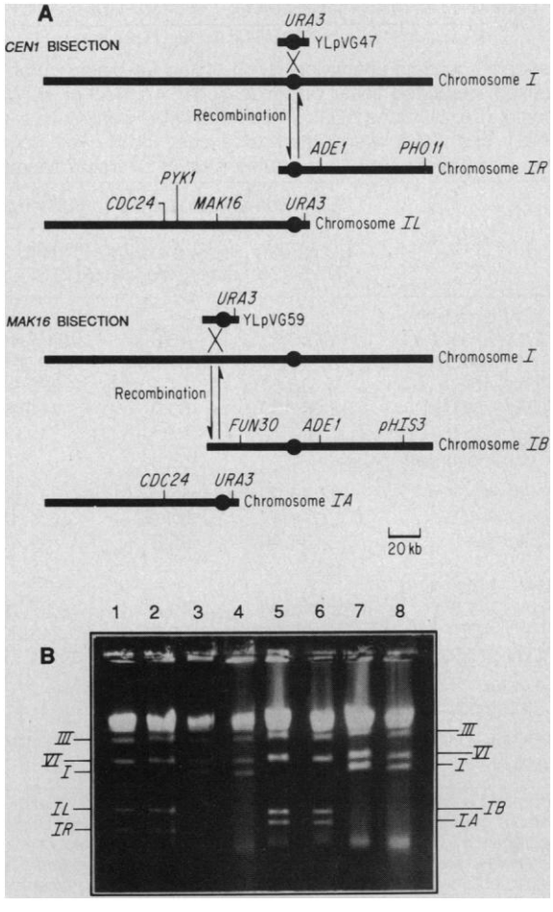

Fig. 1. Formation and physical maps of chromosome *I* bisections. (**A**) Chromosome *I* was bisected at *CEN1* and at *MAK16* by homologous recombination with a small linear plasmid [YLpVG47 or YLpVG59 (*9*)]. Homologous recombination between chromosome fragments was also used to reconstitute intact chromosomes and eject linear plasmids making cells Ura3$^-$ and able to grow on medium containing 5-fluoro-orotic acid (*9*). Physical location of markers shown on bisected chromosomes (*5, 25*). Linear plasmids drawn 1.5× larger than scale. (**B**) Representative electrophoretic karyotypes of chromosome *I* bisections. We separated chromosomes by PFGE using 25-s pulses to maximize separation of small chromosomes (*9*). Roman numerals refer to chromosome numbers. Lanes 1 and 2, haploid parents of strain DB1 containing chromosome *I* bisected at *CEN1*; lanes 3 and 4, haploid parents of DB1 control containing reconstituted copies of chromosome *I*; lanes 5 and 6, haploid parents of strain JM32 containing chromosome *I* bisected at *MAK16*; lanes 7 and 8, haploid parents of JM32 control containing reconstituted copies of chromosome *I*. Results with strain AD3 were identical to those of DB1, and results with strain JM31 were identical to those of JM32.

presence of one shortened chromosome may be sufficient to affect recombination.

In summary, reciprocal recombination rates increased when chromosomes were shortened and decreased when chromosomes were lengthened. Because these effects were seen in four different constructs all involving different chromosomal breakpoints, it is unlikely they were caused by the creation of some new sequence context that coincidentally stimulated or inhibited recombination on an entire chromosome. These results also could not be caused by differences in strain backgrounds because most comparisons were between isogenic strains and the rest were between congenic strains. Because there was increased recombination in both the *CEN1* telocentric and the *MAK16* metacentric bisections, it is also unlikely centromere location was responsible. Finally, sporulation occurred to the same extent and spore viability was always high, making it unlikely a selected population of asci was examined. Thus, our results clearly demonstrate that reciprocal recombination is directly affected by chromosome size. Furthermore, these results suggest it is unlikely that small yeast chromosomes had to evolve specific sequences that enable them to recombine at high rates.

Similar size-dependent control of recombination might exist in *Neurospora crassa* and in humans where small chromosomes appear to recombine at higher rates than large ones (*15, 16*). This control may be especially important for the small homologous pseudoautosomal region of human X and Y chromosomes, which are known to recombine with each other at extremely high rates (*17*). Finally, because reciprocal recombination rates change as a function of chromosome size, equating physical and genetic distances on different sized chromosomes must be done with caution.

We propose that the size-dependent control of recombination is involved in ensuring that each pair of homologous chromosomes undergoes crossing-over during meiosis. In this regard, the frequency of finding asci that did not undergo recombination (the zero-crossover class) within large intervals on chromosome *I* was lowered for all bisected chromosomes. For example, the zero-crossover class for *FUN30-ADE1-pHIS3*, which spans most of chromosome *IB*, was 16% when it was contained on the full-length control chromosomes but dropped to <0.1% for the bisection (*18*). Thus, small increases in recombination rates were dramatically connected to the ability to undergo at least one crossover.

Our observations suggest the existence of a mechanism for controlling recombination that responds directly to chromosome size. This mechanism could function by stimulating recombination on small chromosomes or inhibiting it on large ones. One possibility is that chiasma interference is involved. Chiasma interference inhibits further crossing-over in regions that have already undergone exchange. We observed

Table 1. Decreasing the size of chromosome *I* increases reciprocal recombination rates. Asci from diploids containing either homozygous bisected or homozygous full-length copies of chromosome *I* were analyzed as described (*5, 9*). The numbers of asci analyzed were 148, 82, 47, and 154 for strains DB1, AD3, JM31, and JM32, respectively, and 254, 87, 58, and 218 for the reconstituted full-length chromosome *I* derivatives of DB1, AD3, JM31, and JM32, respectively. Recombination map distance equals 100 [T + 6NPD]/2 × total asci or 100[SDS]/2 × total asci (*20*). Spore viability was greater than 90%. Tetrad data from the small number of three viable-spored asci were consistent with data from four viable-spored asci and combined. Relevant genotypes of strains homozygous for chromosome *I* bisections:

DB1 *MATa* *CDC24* *PYK1* [YLpVG47*URA3*] *ade1::HIS3* *pho11::LEU2* *TRP1* *leu2-3,112* *his3-11,15* *ura3-1*
MATα *cdc24-4* *cdc19-1** [YLpVG47*URA3*] *ADE1* *PHO11* *trp1* *leu2-3,112* *his3-11,15* *ura3-1*

AD3 *MATa* *PYK1* *MAK16* [YLpVG47*URA3*] *ADE1* *PHO11* *TRP1* *leu2-3,112* *his3-11,15* *ura3-1*
MATα *pyk1-102* *mak16-1* [YLpVG47*URA3*] *ade1::HIS3* *pho11::LEU2* *trp1* *leu2-3,112* *his3-11,15* *ura3-1*

JM32 *MATa* *CDC24* [YLpVG59*URA3*] *FUN30* *ADE1* *pHIS3*† *trp1* *leu2-3,112* *his3-11,15* *ura3-1*
MATα *cdc24-5* [YLpVG59*URA3*] *fun30::LEU2* *ade1* *0* *TRP1* *leu2-3,112* *his3-11,15* *ura3-1*

Isogenic controls containing reconstituted full-length chromosome *I* had identical genotypes but lacked integrated linear plasmids YLpVG47*URA3* or YLpVG59*URA3* (*9*). Results from intervals common to DB1 and AD3 or JM31 and JM32 were virtually identical and combined. Genotypes of JM31 and JM32 were identical except JM31 was homozygous for *CDC24*. Bisection and reconstitution for JM31 were demonstrated by electrophoretic karyotyping only (*18*).

Interval	Bisection chromosomes		Full-length chromosomes		*p*‖	Strain
	PD:NPD:T FDS:SDS‡	Recombination map distance	PD:NPD:T FDS:SDS‡	Recombination map distance§		
CEN1 bisection						
CDC24-PYK1	93:0:43	15.8	194:0:46	9.6 (10.7)	0.010	DB1
PYK1-MAK16	26:10:31	67.9	40:0:32¶	22.2 (ND)	0.001	AD3
CEN1-ADE1	186:31	7.1	285:51	7.6 (4.0)	0.868	DB1/AD3
ADE1-PHO11	52:26:139	68.0	75:11:245	47.0 (44.7)	0.002	DB1/AD3
Total for chromosome *I*		158.8		86.4 (80.0)		
PYK1-ADE1	22:16:92	Unlinked	60:23:160	61.3 (57.2)		DB1
MAK16-ADE1	11:14:41	Unlinked	36:4:42	40.2 (40.4)		AD3
CEN3-MAT	34:46	28.8	39:48	27.6 (25.3)	0.883	AD3
MAK16 bisection						
FUN30-ADE1	82:11:100	43.0	148:5:118	27.3 (ND)	0.007	JM32/JM31
CEN1-ADE1	168:26	6.7	242:30	5.5 (4.0)	0.527	JM32/JM31
ADE1-pHIS3	64:11:115	47.6	89:4:177	37.2 (33.5)	0.027	JM32/JM31
Total for chromosome *IB*#		90.6		64.5 (60.9)		
CDC24-FUN30	22:31:92	Unlinked	75:5:134	38.3 (ND)		JM32
CEN3-MAT	78:112	29.5	121:152	27.8 (25.3)	0.546	JM32/JM31

**cdc 19-1* is an allele of *PYK1* (*21*). †*pHIS3* is a plasmid insertion (*22*). *O* indicates no insertion. ‡PD:NPD:T, number of parental ditype:nonparental ditype:tetratye asci or FDS:SDS, number of first division:second division segregation asci scored with respect to *TRP1*. §Published values (*4, 23, 24*) shown in parentheses. ND, not determined previously. ‖Probability observed differences were due to chance; calculated from contingency χ^2 values obtained from PD:NPD:T or FDS:SDS data. ¶Not scored in all asci. #*CEN1-ADE1* not included because this interval is contained within *FUN30-ADE1*.

Table 2. Gene conversions in strains homozygous for either bisected or full-length copies of chromosome *I*. The number (Asci) and percentage of asci having gene conversions for each marker for the analyses described in Table 1 are shown.

Marker	Bisection chromosomes		Full-length chromosomes		Strain
	Asci	(%)	Asci	(%)	
CDC24	1	0.7	2	0.8	DB1
	8	5.2	3	1.4	JM32
PYK1	11	7.5	12	4.7	DB1
	8	9.8	5	5.7	AD3
MAK16	2	2.4	3	3.4	AD3
FUN30	1	0.5	0	0	JM31/JM32
ADE1	12	5.2	0	0	DB1/AD3
	7	3.5	4	1.4	JM31/JM32
pHIS3	4	2.0	2	0.7	JM31/JM32
PHO11	2	0.9	8	2.3	DB1/AD3
TRP1	3	1.4	4	1.2	DB1/AD3
	0	0	2	0.7	JM31/JM32
MAT	1	1.1	0	0	AD3
	0	0	0	0	JM31/JM32

Table 3. Increasing the size of the chromosome *I* DNA molecule by translocation decreases recombination rates. Diploids containing either homozygous translocations or homozygous normal chromosomes were analyzed as described in Table 1. The numbers of asci analyzed were 181, 111, 116, and 102 for DH11, DH12, DH13, and DH19, respectively. Relevant genotypes of reciprocal translocation homozygotes:

DH11 *MATa ade1 cdc15-1 pho11:LEU2* [*URA3HIS3*] *his3-11,15 ura3-1 leu2-3,112 TRP1*
MATα ADE1 CDC15 PHO11 [*URA3 HIS3*] *his3-11,15 ura3-1 leu2-3,112 trp1*

DH12 *MATa cdc24-4 cdc19-1* FUN30* [*URA3 HIS3*] *his3-11,15 ura3-1 leu2-3,112 TRP1*
MATα CDC24 PYK1 fun30::LEU2 [*URA3 HIS3*] *his3-11,15 ura3-1 leu2-3,112 trp1*

Congenic normal strains (DH19 and DH13) were identical but lacked the integrated [*URA3 HIS3*] used to construct and mark the translocation. Footnotes and abbreviations are explained in Table 1.

Interval	*I-II* and *II-I* translocation chromosomes		Normal chromosomes		*p*‖	Strain
	PD:NPD:T FDS:SDS‡	Recombination map distance	PD:NPD:T FDS:SDS‡	Recombination map distance§		
CDC24-PYK1	86:0:14	7.0	78:1:22	13.9 (10.7)	0.05	DH12/DH13
PYK1-FUN30	60:0:38	19.4	46:3:57	35.4 (ND)	0.02	DH12/DH13
CEN1-ADE1	152:21	6.1	93:7	3.5 (4.0)	0.25	DH11/DH19
ADE1-CDC15	160:0:5	1.5	95:0:4	2.0 (2.2)	0.93	DH11/DH19
CDC15-PHO11	67:1:102	31.8	35:5:57	44.9 (42.5)	0.05	DH11/DH19
Total for chromosome *I*		65.8		99.7		
MAT-CEN3	69.88	28.0	46:55	27.2 (25.3)	0.90	DH11/DH19
MAT-CEN3	46:58	27.9				DH12

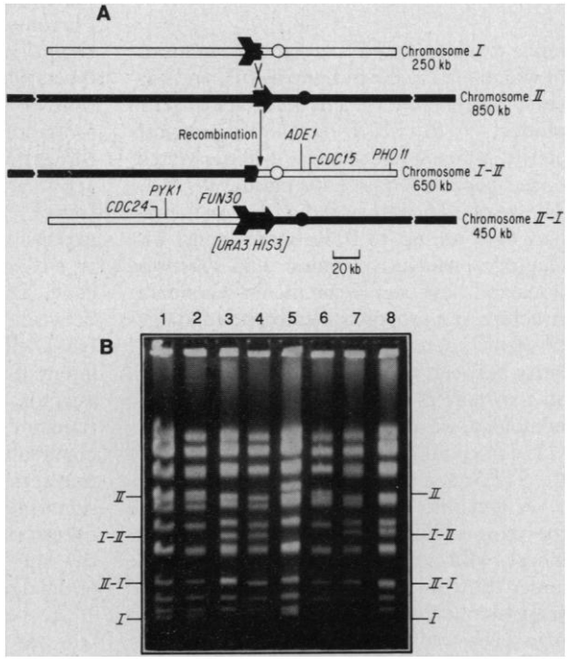

Fig. 2. (**A**) Formation and physical map of the chromosome *I*–chromosome *II* reciprocal translocation. A YIp5-based plasmid containing *URA3*, a 0.9-kb 3′ deletion fragment of the *HIS3* gene (arrow tail), and a 2.0-kb Eco RI target fragment from chromosome *I* [isolated from pLF31 (*26*)] was homologously integrated into strain YNN285 (*11*) 18 kb to the left of *CEN1*. This strain contained a 1.2-kb 5′ deletion fragment from the *HIS3* gene (arrowhead) integrated near *GAL1* on chromosome *II*. The two *HIS3* fragments partially overlapped so that mitotic recombination between them produced a functional *HIS3* gene (complete arrow) and a chromosome *I-II* reciprocal translocation. His$^+$ colonies were selected and screened by PFGE to identify those containing the electrophoretic karyotype indicative of the translocation. Gels were analyzed by blot hybridization to confirm chromosomal identity (*18*). Translocation strains were crossed to normal strains containing chromosome *I* markers. These crosses gave spore viability patterns indicative of translocation heterozygotes (*27*). Physical locations of markers are shown. [*URA3 HIS3*] indicates the *URA3* gene is adjacent to the 5′ end of the reconstituted *HIS3* gene. The *HIS3* gene and gene-fragments are not drawn to scale. (**B**) Electrophoretic karyotypes of strains containing translocations or normal chromosomes. Roman numerals refer to normal and translocation chromosomes. Chromosome *II-I* comigrated with chromosome *IX* (note relative band intensities). Lanes 1 and 2, haploid parents of DH13, the congenic control containing normal chromosomes; lanes 3 and 4, haploid parents of strain DH12 containing the chromosome *I-II* translocation; lanes 5 and 6, haploid parents of DH20, the congenic control containing normal chromosomes; lanes 7 and 8, haploid parents of strain DH11 containing the chromosome *I-II* translocation.

Table 4. Gene conversions in strains homozygous for either *I-II* and *II-I* translocations or normal copies of chromosome *I*. The number (Asci) and percentage of asci having gene conversions for each marker for the analyses described in Table 3 are shown.

Marker	Chromosomes				Strain
	I-II and *II-I* translocation		Normal		
	Asci	(%)	Asci	(%)	
CDC24	2	1.8	5	4.3	D12/DH13
PYK1	10	9.0	9	7.8	DH12/DH13
FUN30	1	0.9	1	0.9	DH12/DH13
MAT	0	0			DH12
ADE1	6	3.3	1	1.0	DH11/DH19
CDC15	9	5.0	2	2.0	DH11/DH19
PHO11	2	1.1	1	1.0	DH11/DH19
TRP1	2	1.1	1	1.0	DH11/DH19
MAT	0	0	0	0	DH11/DH19

that tetrads with double crossovers (NPDs) were disproportionately (two- to tenfold) more abundant for the bisected chromosomes and disproportionately (three- to fivefold) less abundant for the larger translocated chromosomes compared to normal length chromosomes. These changes suggest that the amount of chiasma interference increases with chromosome size (*19*). This observation is consistent with the idea that this negative control mechanism is somehow involved in the size-dependent control of meiotic recombination.

REFERENCES AND NOTES

1. B. S. Baker, A. T. C. Carpenter, M. Esposito, R. E. Esposito, L. Sandler, *Annu. Rev. Genet.* **10**, 53 (1976).
2. T. D. Petes and D. Botstein, *Proc. Natl. Acad. Sci. U.S.A.* **74**, 5091 (1977).
3. A. J. Link and M. V. Olson, *Genetics* **127**, 681 (1991).
4. R. K. Mortimer, D. Schild, C. R. Contoupoulou, J. A. Kans, *Yeast* **5**, 321 (1989).
5. D. B. Kaback, H. Y. Steensma, P. de Jonge, *Proc. Natl. Acad. Sci. U.S.A.* **86**, 3694 (1989).
6. L. Clarke and J. Carbon, *Nature* **287**, 504 (1980).
7. L. S. Symington and T. D. Petes, *Mol. Cell. Biol.* **8**, 595 (1988).
8. A. Nicolas, D. Treco, N. P. Schultes, J. W. Szostak, *Nature* **338**, 35 (1989).
9. V. Guacci and D. B. Kaback, *Genetics* **127**, 475 (1991).
10. K. G. Coleman, H. Y. Steensma, D. B. Kaback, J. R. Pringle, *Mol. Cell. Biol.* **6**, 4516 (1986).
11. M. T. Fasullo and R. W. Davis, *Proc. Natl. Acad. Sci. U.S.A.* **84**, 6215 (1987).
12. E. J. Lambie and G. S. Roeder, *Genetics* **109**, 303 (1986).
13. This interval contains approximately 75 kb of DNA (*4*), so it is not appreciably affected by centromere inhibition.
14. R. T. Surosky and B. K. Tye, *Genetics* **119**, 273 (1988).
15. J. King, personal communication.
16. According to data obtained in N. E. Morton, *Proc. Natl. Acad. Sci. U.S.A.* **88**, 7474 (1991).
17. H. J. Cooke, W. R. A. Brown, G. A. Rappold, *Nature* **317**, 687 (1985).

18. J. Mahon and D. B. Kaback, unpublished observations.
19. D. B. Kaback, unpublished observations.
20. D. D. Perkins, *Genetics* **34**, 607 (1949).
21. D. B. Kaback *et al.*, *Genetics* **108**, 67 (1984).
22. H. Y. Steensma, P. deJonge, A. Kaptein, D. B. Kaback, *Curr. Genet.* **16**, 131 (1989).
23. R. K. Mortimer and D. Schild, *Microbiol. Rev.* 44, 519 (1980).
24. _____, *ibid.* **49**, 181 (1985).
25. M. W. Clark *et al.*, *Yeast* **8**, 133 (1992).
26. W. L. Whyte, L. L. Koepp, J. L. Lamb, J. C. Crowley, D. B. Kaback, *Gene* **95**, 65 (1990).
27. D. D. Perkins, *Genetics* **77**, 459 (1974).
28. We thank A. Deshpande and C. Myers for performing some experiments; M. Fasullo, A. Barton, and B. K. Tye for strains and plasmids; R. K. Mortimer and J. King for valuable discussions; and F. Stahl and M. Brandriss for comments on the manuscript. Supported by grants from the NSF and the New Jersey Commission on Cancer Research.

8 October 1991; accepted 21 February 1992

Functional Complementation of Yeast *ste6* by a Mammalian Multidrug Resistance *mdr* Gene

Martine Raymond,* Philippe Gros, Malcolm Whiteway, David Y. Thomas

Multidrug resistance in mammalian tumor cells is associated with the overexpression of *mdr* genes encoding P-glycoproteins, which function as drug efflux pumps. A yeast homolog of *mdr*, *STE6*, mediates export of a-factor mating peptide. Yeast *MAT*a cells carrying a *ste6* deletion produce no extracellular a-factor and therefore are defective in mating. Expression of a complementary DNA for the mouse *mdr3* gene in a yeast *ste6* deletion strain restored ability to export a-factor and to mate. A mutation (a serine to phenylalanine substitution at amino acid 939) known to affect the activity of the *mdr3* gene product abolished its ability to complement the yeast *ste6* deletion. Thus, functions of P-glycoproteins in normal mammalian cells may include the transmembrane export of endogenous peptides.

Multidrug resistance (MDR) in cultured cells in vitro and in tumor cells in vivo is associated with the overexpression of members of a small gene family, designated *mdr* or *pgp*, that codes for membrane P-glycoproteins (Pgps) (*1*). Pgps are composed of two homologous halves; each half consists of six predicted transmembrane domains and an intracellular loop with a consensus adenosine triphosphate (ATP) binding motif (*1*). Pgps apparently function as energy-dependent drug efflux pumps that reduce the intracellular accumulation of a wide variety of chemotherapeutic drugs in resistant cells (*2*). In addition, Pgps display a specific pattern of expression in normal tissues, implicating Pgps in normal transport of endogenous cellular substrates (*3*). If so, these normal substrates have yet to be identified.

Pgps are members of a superfamily of evolutionarily conserved transport proteins (*4*). This superfamily includes the *pfmdr1* gene product of *Plasmodium falciparum* associated with chloroquine resistance (*5*), the cystic fibrosis (CF) transmembrane conductance regulator (CFTR) protein, mutations in which lead to CF in humans (*6*), and the yeast *Saccharomyces cerevisiae STE6* gene product (*7, 8*), which mediates the export of the a-factor pheromone, a farnesylated dodecapeptide required for mating (*9, 10*). The yeast *STE6* gene product and mammalian Pgps are up to 57% homologous, including conservative amino acid substitutions and have similar predicted secondary structure and proposed membrane topology (*7, 8*). To determine if the structural similarity between the yeast and the mammalian transporters translates into a functional homology, we asked if the mouse *mdr3* gene (*11, 12*) could complement the function of the *STE6* gene in a yeast *ste6* mutant strain.

A genomic DNA fragment containing the yeast *STE6* gene and a cDNA for the mouse wild-type *mdr3* gene were placed under the control of the promoter for the yeast alcohol dehydrogenase gene on the high copy vector pVT, yielding plasmids pVT-STE6 and pVT-MDR3S, respectively (*13*). In addition, a mutant *mdr3* derivative with a serine to phenylalanine substitution at amino acid position 939 was subcloned into pVT and the resulting construct designated pVT-MDR3F (*13*). The Ser^{939} to Phe^{939} substitution within predicted transmembrane domain 11 (TM-11) of the *mdr3* gene product decreases the activity and modifies the substrate specificity of this transporter for drugs of the MDR spectrum (*12*). These three constructs, along with plasmid pVT as negative control, were transformed into yeast JPY201 *MAT*a Δ*ste6*::*HIS3* cells, in which 70% of the *STE6* gene was deleted and replaced with the yeast *HIS3* gene (*7*). Thus, JPY201 cells do not export a-factor and are sterile (*7*).

The activity of the *STE6* or *mdr3* gene products was measured by the ability of transformed JPY201 cells to arrest growth of *MAT*α cells and to mate, functions dependent on extracellular a-factor pheromone production (*14*). In a growth arrest assay (Fig. 1), production of pheromone by a patch of cells inhibits growth of a lawn of cells of the opposite mating type, resulting in a clear zone or halo surrounding the patch (*15*). Control JPY201 cells transformed with pVT [JPY201(pVT)] were defective in the production of extracellular a-factor (*7*), but JPY201 cells transformed with pVT-STE6 [JPY201(pVT-STE6)] or pVT-MDR3S [JPY201(pVT-MDR3S)] produced a zone of growth inhibition of significant size, indicating their ability to export substantial amount of a-factor pheromone (*16*). In contrast, cells transformed with pVT-MDR3F [JPY201(pVT-MDR3F)] produced no discernible halo.

The ability of JPY201 transformants to mate was also assayed (Fig. 2 and Table 1). Pheromone production triggers mating between haploid cells of opposite mating types, which leads ultimately to the formation of diploid cells (*14*). Thus, diploid formation provides a sensitive measure for the extracellular production of biologically active a-pheromone (*10*). The mating defect of JPY201(pVT) cells was corrected by expression of either the *STE6* or the wild-type *mdr3* gene but not by the mutant *mdr3* gene. The difference in mating efficiencies between JPY201(pVT-STE6) and JPY201-(pVT-MDR3S) cells may reflect their differential ability to transport extracellular a-factor, a likely consequence of the evolutionary distance between the yeast and the mammalian transporters expressed in these transformants. The construction and functional testing of chimeric molecules between *STE6* and *mdr3* should help to identify the protein domains responsible for optimal a-factor transport by STE6.

To verify that the MDR3(Phe^{939}) protein was appropriately expressed and targeted, we prepared cell membranes from JPY201 transformants and analyzed them by immunoblotting for the presence of the wild-type and mutant *mdr3* gene products (Fig. 3). JPY201(pVT-MDR3S) and JPY201(pVT-MDR3F) cells produce similar amounts of immunoreactive MDR3(Ser^{939}) and MDR3(Phe^{939}) proteins, which are not detected in control cells transformed with plasmid pVT. The mouse *mdr3* gene products expressed in yeast cells display a faster

M. Raymond, M. Whiteway, D. Y. Thomas, National Research Council of Canada, Biotechnology Research Institute, Montreal, Quebec, Canada H4P 2R2, and Department of Biology, McGill University, Montreal, Quebec, Canada H3A 1B1.
P. Gros, Department of Biochemistry, McGill University, Montreal, Quebec, Canada H3G 1Y6.

*To whom correspondence should be addressed.